Volume 15
Number 4
21 February 2024
Pages 1723-2330

Food & Function

Linking the chemistry and physics of food with health and nutrition

rsc.li/food-function

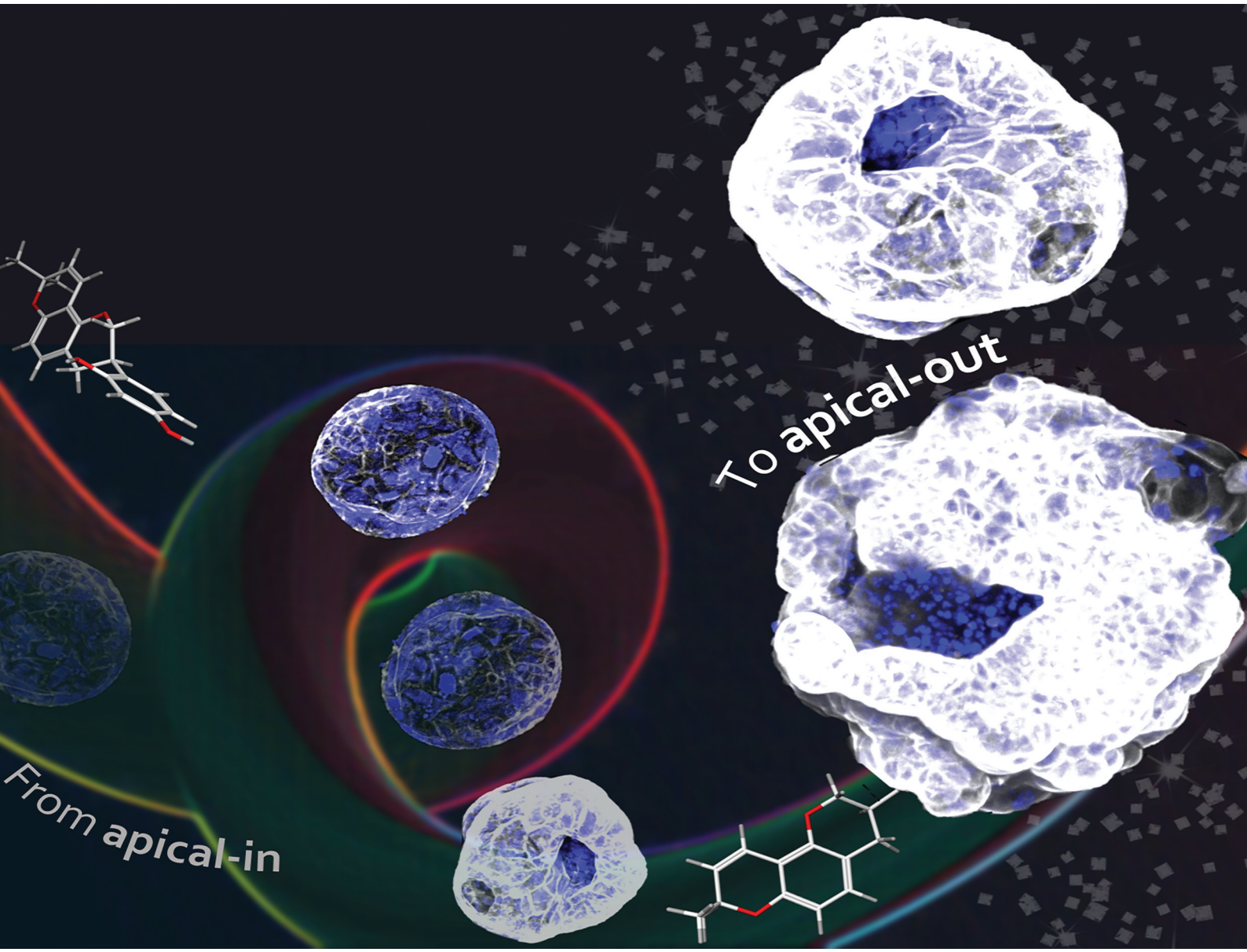

ISSN 2042-650X

ROYAL SOCIETY OF CHEMISTRY

PAPER

Jocelijn Meijerink *et al.*
Switching the polarity of mouse enteroids affects the epithelial interplay with prenylated phenolics from licorice (*Glycyrrhiza*) roots

Food & Function

ROYAL SOCIETY OF CHEMISTRY

PAPER

View Article Online
View Journal | View Issue

Cite this: *Food Funct.*, 2024, **15**, 1852

Switching the polarity of mouse enteroids affects the epithelial interplay with prenylated phenolics from licorice (*Glycyrrhiza*) roots†

Sarah van Dinteren,[a,b] Carla Araya-Cloutier,[b] Edyta Robaczewska,[a] Mellody den Otter,[a] Renger Witkamp,[a] Jean-Paul Vincken[b] and Jocelijn Meijerink*[a]

The utility of 3D-small intestinal organoid (enteroid) models for evaluating effects of *e.g.* food (related) compounds is limited due to the apical epithelium facing the interior. To overcome this limitation, we developed a novel 3D-apical-out enteroid model for mice, which allows apical exposure. Using this model, we evaluated the effects on the enteroids' intestinal epithelium (including cytotoxicity, cell viability, and biotransformation) after exposure to glabridin, a prenylated secondary metabolite with antimicrobial properties from licorice roots (*Glycyrrhiza glabra*). Apical-out enteroids were five times less sensitive to glabridin exposure compared to conventional apical-in enteroids, with obtained cytotoxicities of 1.5 mM and 0.31 mM, respectively. Apical-out enteroids showed a luminal/apical layer of fucose rich mucus, which may contribute to the protection against potential cytotoxicity of glabridin. Furthermore, in apical-in enteroids IC_{50} values for cytotoxicity were determined for licochalcone A, glycycoumarin, and glabridin, the species-specific prenylated phenolics from the commonly used *G. inflata*, *G. uralensis*, and *G. glabra*, respectively. Both enteroid models differed in their functional phase II biotransformation capacity, where glabridin was transformed to glucuronide- and sulfate-conjugates. Lastly, our results indicate that the prenylated phenolics do not show cytotoxicity in mouse enteroids at previously reported minimum inhibitory concentrations (MICs) against a diverse set of Gram positive bacteria. Altogether, we show that apical-out enteroids provide a better mimic of the gastrointestinal tract compared to conventional enteroids and are consequently a superior model to study effects of food (related) compounds. This work revealed that prenylated phenolics with promising antibacterial activity show no harmful effects in the GI-tract at their MICs and therefore may offer a new perspective to control unwanted microbial growth.

Received 20th July 2023,
Accepted 21st November 2023

DOI: 10.1039/d3fo02961a

rsc.li/food-function

1. Introduction

Prenylated (iso)flavonoids and chalcones are phenolic metabolites with promising antimicrobial properties found in plants from the Fabaceae family, such as licorice (including *Glycyrrhiza glabra*, *G. inflata*, and *G. uralensis*).[2–5] Natural antimicrobials, including prenylated phenolics, are highly sought-after as alternatives for existing antimicrobials due to *e.g.* increased antibiotic resistance and a general increased interest in minimal processed and "natural" products.[6,7] Attachment of a prenyl moiety (*e.g.* 3-methyl-2-butene) to a phenolic backbone is known to increase its antibacterial potency, partly due to the increased hydrophobicity conferred to the molecule.[8,9] This increased hydrophobicity by prenylation is thought to enhance the interaction, permeabilization, and/or disruption of bacterial membranes, leading to increased antibacterial activity.[8,9] At the same time, these interactions of prenylated phenolics with biological targets, including cell membranes, raise concerns regarding their safety for consumption as food components. Several studies have shown that prenylated phenolics induce cytotoxicity and reduce cell viability in cell lines.[10–13] For example, prenylated flavanones isolated from propolis have been shown to reduce cell proliferation in mouse-derived cell lines (including 26-L5 colon, B16–Bl6 melanoma, and Lewis lung cell lines), with IC_{50} values ranging from 14–64 μM.[14] Moreover, we have previously shown that the prenylated phenolics glabridin (glab: single ring prenylated isoflavan from *G. glabra*), licochalcone A (licoA: single chain prenylated chalcone from *G. inflata*), and glycycoumarin

[a]*Division of Human Nutrition and Health, Wageningen University, P.O. box 17, 6700 AA Wageningen, The Netherlands. E-mail: jocelijn.meijerink@wur.nl*
[b]*Laboratory of Food Chemistry, Wageningen University, P.O. box 17, 6700 AA Wageningen, The Netherlands*

† Electronic supplementary information (ESI) available. See DOI: https://doi.org/10.1039/d3fo02961a

(glycy: single chain prenylated 3-arylcoumarin from *G. uralensis*) displayed cytotoxicity in (human-derived) Caco-2 cells at 50 μg mL^{-1} (136–154 μM), and reduced cell viability at 25 μg mL^{-1} for glab (77 μM) and glycy (68 μM), and at 12.5 μg mL^{-1} for licoA (37 μM) (Fig. 1).[1]

Although colon-derived cell lines, such as Caco-2, are widely used models to evaluate *in vitro* cytotoxicity, they have significant limitations as models since they do not accurately replicate the complex *in vivo* environment of the intestine and exhibit various genotypic and phenotypic functional aberrations.[15–18] This creates a strong demand for *in vitro* models that are better suited to study the interactions between molecules present in the gastrointestinal tract such as nutrients, bioactive substances, and metabolites, with the intestinal epithelium. Small intestinal organoids or enteroids, self-sustained non-cancerous mini-guts are grown from pluripotent Lgr5+ stem cells and show good resemblance with the *in vivo* architecture. Furthermore, they contain all different epithelial cells, including absorptive enterocytes, goblet cells, enteroendocrine cells, and Paneth cells.[19,20] Consequently, epithelial cells derived from enteroids were shown to represent a genotypically and phenotypically superior model when compared to Caco-2 cells.[18] In the conventional apical-in model, the enteroids are embedded in a 3D extracellular protein matrix (ECM) which is surrounded by culture medium with appropriate growth factors. The apical or mucosal surface is enclosed within the enteroid and the basolateral surface is facing outwards,[19] making this model less attractive for *e.g.* nutrient exposure experiments.[21] In order to access the apical surface of 3D-enteroids, Co *et al.* recently developed a method to generate suspension cultures of human 3D enteroids, without the use of ECM, with reversed polarity, in such a way that the apical surface faces outward (apical-out).[22] In comparison with 3D apical-in enteroids, apical-out enteroid suspensions are advantageous in *i.e.* pharmacological and food research, as it makes the luminal site accessible for drugs, metabolites or food components, without the need of micro-injection.[21,23] Moreover, the apical surface releases secretions such as mucins that make up the core of the mucus layer which acts, amongst others, as a protective physical barrier from the luminal content.[24,25] Apical-out enteroids recapitulate the properties and functions of the native intestinal epithelium, including barrier function, absorptive, and secretory properties.[21,22]

In this study, we developed a mouse apical-out enteroid model in which the intestinal epithelium is surrounded by a mucus layer, wherein cytotoxicity and effects on cell viability of bioactive compounds can be determined. To limit variability, enteroids were created from the inbred C57BL/6 mouse, which is the most widely used strain in biomedical research. This is the first published study, to the best of our knowledge, that describes the development of apical-out mouse enteroids as model to evaluate *in vitro* toxicity of prenylated phenolics. Polarity reversal (from apical-in to apical-out enteroids) was visualized by fluorescence confocal microscopy, in which the nuclei, actin cytoskeleton in the microvilli brush border, and fucose units in the glycoproteins of the mucus layer were stained. With this model, the cytotoxicity and cell viability of glab were determined and compared to those measured in the conventional apical-in enteroid model (in which the basolateral side without mucus layer was stimulated, *e.g.* representative for impaired barrier function). Additionally, the cytotoxicity of three prenylated phenolics (glab, licoA, and glycy) was compared in apical-in enteroids. In order to assess whether the intestinal cytotoxicity observed was derived from the prenylated phenolics and/or their metabolites, we also evaluated the intestinal biotransformation of glab, licoA, and glycy, as it has been shown previously that glab was glucuronidated in rat intestinal microsomes and human colon cell lines (Caco-2).[26]

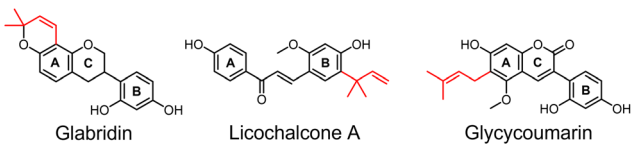

Fig. 1 Species-specific compounds glabridin (glab), licochalcone A (licoA), and glycycoumarin (glycy). Molecular structures of the main species-specific compounds glab (ring prenylated isoflavan from *G. glabra*), licoA (chain prenylated chalcone from *G. inflata*), and glycy (chain prenylated 3-arylcoumarin from *G. uralensis*). Prenyl group is indicated in red.

2. Experimental

2.1. Materials

Glabridin (glab) (≥97.0%) was purchased from Wako (Osaka, Japan); licochalcone A (licoA) (≥96.0%), bovine serum albumin, and Triton™ X-100 from Sigma-Aldrich (St Louis, MO, USA); glycycoumarin (glycy) (≥98.0%) from ChemFaces (Wuhan, China; confirmed by RP-UHPLC-PDA-FT-MS^n); Phosphate Buffered Saline (PBS), GlutaMAX™ supplement, TrypLE™ Express enzyme reagent, and bovine serum albumin (BSA) were purchased from Thermo Fisher Scientific Gibco (Waltham, Massachusetts, USA); DMEM/F12 with 15 mM HEPES buffer, Gentle Cell Dissociation Reagent (GCDR), Intesticult™ mouse organoid growth medium (mIC), and Intesticult™ human organoid growth medium (hIC) were purchased from STEMCELL Technologies (Vancouver, Canada); Matrigel® growth factor reduced basement membrane matrix phenol red-free and penicillin/streptomycin (P/S) solution 100× were purchased from Corning Incorporated (Somerville, Massachusetts, USA). ACN containing 0.1% (*v*/*v*) formic acid (FA), water containing 0.1% (*v*/*v*) FA were purchased from Biosolve (Valkenswaard, The Netherlands); dimethyl sulfoxide (DMSO) was purchased from Merck Millipore (Billerica, MA, USA). Water (MQ) for other purposes than UHPLC was prepared using a Milli-Q water purification system (Merk Millipore).

2.2. Jejunal enteroids

Mouse enteroids were generated from jejunal tissue of C57BL/6 mice, which was approved by the Animal Ethics Committee of Wageningen University and Research (WUR), Wageningen, The Netherlands. Animal handling was according to Dutch law on use of laboratory animals. The enteroids were kept frozen in liquid nitrogen until use. For the experiments, frozen mouse jejunal enteroids (~200 enteroids/cryovial) were thawed in an incubator at 37 °C. Enteroids were mixed with DMEM/F12 (supplemented with 1% (*w*/*v*) BSA, 15 mM HEPES buffer solution, GlutaMAX supplement, and 1% (*v*/*v*) P/S, abbreviated as DMEM/F12) and centrifuged at 200*g* for 5 min at 4 °C. Pellet was mixed with Matrigel (Corning Matrigel® growth factor reduced basal membrane matrix, AZ, USA) (1 : 1 diluted with DMEM/F12) and 35 μL domes were plated on a 24-wells plate. Per well 500 μL mIC was added. Medium was changed every two days. Enteroids were passaged every 5–6 days in a 1 : 7 to 1 : 8 split ratio.

2.3. Generation of 3D apical-out jejunal enteroids

Apical-out jejunal enteroids were generated as described elsewhere,[21,22] with the following adaptations. In brief, apical-in mouse enteroids (approximately 200 enteroids per dome) were cultured in a 3D system with Matrigel® for at least 1 passage with hIC for 3–4 days. To generate apical-out enteroids, Matrigel® with enteroids was collected with GCDR and incubated (in prewetted tubes with anti-adherence solution (STEMCELL)) for 15 min at 4 °C with continuous agitation. The enteroid suspension was centrifuged at 200*g* for 2 min at 4 °C. Pellet (containing enteroids) was washed with DMEM/F12 twice, to completely remove Matrigel® (residual Matrigel® leads to inhibition of polarity reversal). Enteroids were resuspended in hIC in ultra-low binding culture plates (Corning), and incubated at 37 °C with 5% CO_2. The morphology of enteroids was checked and monitored under a microscope daily to follow polarity reversal (see section 2.4). Human organoid growth medium was changed every 2 days. Enteroids were passaged from 3D apical-in to apical-out in a 1 : 2 split ratio for cytotoxicity measurements and in a 1 : 1 split ratio for cell viability (WST-1, see section 2.6) measurements. Stimulation experiments in apical-out enteroids were performed after full polarity reversal, which was 48 h after Matrigel® removal.

2.4. Evaluation of polarity reversal by F-actin fluorescence staining and mucosal fucose staining

Jejunal enteroids (grown for one passage in hIC) were collected (after Matrigel® removal at t = 0 h, at 24 h, 48 h, and 72 h after polarity reversal) and fixed with 3.7% formaldehyde (MeOH free) solution in PBS for 45 min at RT and permeabilized in PBS with 5% BSA and 2% Triton™ X-100 for 60 min at RT. Fucose units in the mucus layer were stained with *Ulex Europaeus* Agglutinin I conjugated to rhodamine (UEA-1) (Invitrogen™, Waltham, MA, United States), F-actin with ActinRed™ 555 (ReadyProbes™ Reagent, Invitrogen™) or AlexaFluor™ 660 Phallaoidin (Invitrogen™), and nuclei with DAPI dilactate (Invitrogen™), according to manufacturer's instructions. In brief, fixed and permeabilized enteroids in suspension were washed three times with immunofluorescence buffer (PBS with 0.1% (*w*/*v*) BSA, 0.2% (*v*/*v*) Triton™ X-100, and 0.1% (*v*/*v*) Tween®-20) (centrifuged at 200*g* for 2 min at RT), and stained with UEA-1 and incubated 30–60 min at RT. Enteroids were subsequently stained with F-actin and incubated for 25 min at RT, after which DAPI was added and the enteroids were further incubated for 15 min. The enteroid suspension was washed and resuspended in PBS, after which the enteroids were imaged with an inverted microscope (Leica DMil, Leica Biosystems, Wetzlar, Germany) equipped with a Leica EL6000 fluorescence external light source (Leica Biosystems). For confocal microscopy, the stained enteroid suspension was transferred to a chambered glass coverslip (Ibidi, Gräfelfing, Germany), after which the enteroids were imaged with a re-scan confocal microscopy (RCM1, confocal.nl, Amsterdam, the Netherlands). Images were analyzed using ImageJ software (version 1.52).

2.5. Cytotoxicity

Cytotoxic effects of glab, licoA, and glycy (1.56–500 μg mL^{-1}) on apical-in enteroids in mIC (passages between 8 and 38), and the cytotoxic effect of glab on apical-out enteroids in hIC (passages between 12–13 and 40–42) were assessed after 4 h, 8 h, and 24 h of exposure, by measuring leakage of intracellular lactate dehydrogenase (LDH) in supernatant and analysis using an LDH cytotoxicity detection kit (Roche Applied Science, Almere, the Netherlands), according manufacturer's instructions. Glab, licoA, and glycy were dissolved in DMSO at 50 mg mL^{-1}. Highest concentration of DMSO in measurements was 1% (*v*/*v*), which did not affect cytotoxicity (data not shown). LDH activity in the supernatant was expressed as percentage of the maximum releasable LDH in enteroids (enteroids treated with 1% Triton™ X-100) and calculated with eqn (1).

$$\text{Cytotoxicity}\,(\%) = \frac{\text{exp.value} - \text{low control}}{\text{high control} - \text{low control}} \times 100 \quad (1)$$

In this equation, exp.value is the UV absorbance at 492 nm (Multiskan Ascent, Thermo Fisher Scientific or Spectramax M2, Molecular Devices, Sunnyvale, CA, USA), low control is the spontaneous LDH release in untreated cells, and high control is the maximum releasable LDH in Triton™-treated enteroids. To correct for the variable number of enteroids per Matrigel® dome, each enteroid dome was treated as its own positive control by taking the total releasable LDH of each well after 24 h incubation (Fig. A1, ESI†). Cytotoxicities and half-maximal inhibitory concentrations (IC_{50}) of glab, licoA, and glycy after 24 h incubation were determined with GraphPad Prism 9.3.1. In brief, for each compound a non-linear regression of log transformed concentrations was performed. Results were expressed as mean values ± standard error of the mean (SEM).

Four hour and 24 h stability of glab, licoA, and glycy in mIC with Matrigel® domes was evaluated. For this, 50 μg mL^{-1} of

each compound was incubated for 4 h and 24 h at 37 °C, after which the compounds were separated and identified with Reversed Phase Ultra High Pressure Liquid Chromatography coupled to Photodiode Array detection and Mass Spectrometry (RP-UHPLC-PDA-MS^n), and quantified based on UV absorbance at 280 nm. UV peaks were integrated using the AVALON integration algorithm with the auto-calc function (Xcalibur 4.1) (see section 2.8.1 and 2.8.2 for RP-UHPLC-PDA-MS^n settings). Seven-point calibration curves (0.1–100 μg mL^{-1}) of glab, licoA, and glycy were used ($R^2 > 0.9999$). Glab, licoA, and glycy were considered stable in mIC, with recoveries of 97 ± 0.39, 95 ± 0.93, and 97 ± 6.3% after 4 h, and 98 ± 0.81, 95 ± 0.57, and 105 ± 8.5% after 24 h incubation, respectively.

2.6. Cell viability by WST-1

Effects on cell viability in apical-out jejunal enteroids after 4 h glab (12.5–500 μg mL^{-1} in hIC) exposure was assessed by measuring cleavage of the tetrazolium salt WST-1 to formazan by cellular mitochondrial dehydrogenases, using a WST-1 cell viability kit (PromoKine, Heidelberg, Germany), according to manufacturer's instructions. Cell viability was expressed as the percentage of the control (mouse small intestinal enteroids in hIC) and calculated with eqn (2).

$$\text{Cell viability}\,(\%) = \frac{\text{exp.value}}{\text{low control}} \times 100 \qquad (2)$$

Here, exp.value is the UV absorbance at 450 nm (Spectramax M2, Molecular Devices, Sunnyvale, CA, USA) and low control is spontaneous cleavage of WST-1 to formazan by mitochondrial dehydrogenases in untreated enteroids. Measured cell viabilities were normalized to total cell content for each well containing enteroids. For this, enteroids were incubated at 37 °C for 20 min with TrypLE™ Express enzyme reagent to dissociate the apical-out enteroids, after which the enzyme was inactivated with FCS. Cells were counted on a TC20 automated cell counter (BioRad, Hercules, CA, USA).

2.7. Cell viability by Live–Dead cell viability assay

Effects on cell viability in apical-in enteroids by glab, licoA, and glycy (1.56–500 μg mL^{-1} in mIC) were assessed after 24 h of incubation with the Live–Dead Cell Viability Assay Kit according to manufacturer's instructions (Merck-Millipore, Burlington, MA, United States). Enteroid medium was aspirated and reagent mixture (containing calcein-AM and propidium iodide) was added. Enteroids were incubated for 1 h and images were recorded with a Leica DMil inverted microscope equipped with a Leica EL6000 fluorescence external light source. Images were analyzed with ImageJ or using Leica LAS X software.

2.8. Biotransformation of glabridin, licochalcone A, and glycyoumarin in apical-in and apical-out jejunal enteroids

Biotransformation of glab in apical-out jejunal enteroids, and of glab, licoA, and glycy in apical-in jejunal enteroids was evaluated after 0 h, 4 h, and 24 h of incubation. For this, enteroids were exposed to 37.5 or 50 μg mL^{-1} glab (116 or 154 μM), 25 μg mL^{-1} licoA (74 μM), and 37.5 μg mL^{-1} glycy (102 μM). These were the highest concentrations tested at which no cytotoxicity (LDH) was observed (data not shown).

2.8.1. Reversed phase liquid chromatography (RP-UHPLC-PDA). Samples were separated on a Thermo Vanquish UHPLC system (Thermo Scientific, San Jose, CA, USA) equipped with a pump, degasser, autosampler, and a PDA detector. The flow rate was 400 μL min^{-1} at a column temperature of 45 °C. Injection volume was 1 μL. Eluents used were water-acidified with 0.1% (*v*/*v*) FA (A) and acetonitrile-acidified with 0.1% (*v*/*v*) FA (B). Samples were separated on an Acquity UPLC C18 (150 mm × 2.1 mm, i.d. 1.7 μM) with a VanGuard (5 mm x 2.1 mm) guard column of the same material (Waters, Milford, USA). The elution program was started by running isocratically at 1% B for 1.09 min, followed by 1.09–38.70 min linear gradient to 70% B, 38.70–39.79 min linear gradient to 100% B, 39.79–45.24 min isocratically at 100% B. Eluent was adjusted to start conditions in 1.09 min, followed by equilibration of 5.45 min. Detection wavelengths for UV-Vis were set in a range between 190 and 680 nm.

2.8.2. Electrospray ionization ion trap mass spectrometry (ESI-IT-MS^n). Mass spectrometric data were acquired using a LTQ Velos Pro linear ion trap mass spectrometer (Thermo Scientific), equipped with a heated ESI probe coupled in-line to the Vanquish UHPLC system. Nitrogen was used as sheath and sweep gas (48 and 2 arbitrary units, respectively). Data were collected in negative ionization (NI) and positive ionization (PI) mode between *m*/*z* 150–1000. Data-dependent MSn analyses were performed by collision-induced dissociation with a normalized collision energy of 35%. MS^n fragmentation was performed on the most intense product ion in the MS^{n-1} spectrum. Dynamic exclusion with a repeat count of 3, repeat duration of 5.0 s, and an exclusion duration of 5.0 s was used to obtain MS^2 spectra of multiple different ions present in full MS at the same time. Ion transfer tube and source heater temperature were 254 °C and 408 °C, respectively. Source voltage was 3.5 (PI) and 2.5 (NI) kV. Data were processed using Xcalibur 4.1 (Thermo Scientific).

2.8.3. Quantification of glabridin and metabolites. Quantification of glab and produced metabolites was based on their UV absorbance at 280 nm. For this, a seven-point (0.1–100 μg mL^{-1}) calibration curve based on the external standards of glab, licoA, and glycy ($R^2 > 0.999$) was used. UV peaks were integrated using the AVALON algorithm with the auto-calc function (Xcalibur 4.1). Metabolites were quantified as glab, licoA, and glycy equivalents.

2.9. qRT-PCR of intestinal cell markers

Apical-in ECM-embedded (grown in mIC and hIC) or apical-out suspended enteroids (grown in hIC) were collected and pelleted by centrifugation at 200*g* for 2 min at RT. RNA was isolated using TRIzol reagent and further purified according manufacturer's protocol (Invitrogen™), after which RNA content and quality was measured with the NanoDrop® ND-1000 spectrophotometer (Isogen Life Science, Utrecht, the Netherlands). Complementary DNA (cDNA) was synthesized

Table 1 qRT-PCR primers. A list of forward and reverse primers that were used to detect different cell type markers in apical-in and apical-out enteroids in this study

Cell marker	Gene	Forward primer	Reverse primer	Ref.
Stem cell	*Lgr5*	GACAATGCTCTCACAGAC	GGAGTGGATTCTATTATTATGG	27
Paneth cell	*Lyz*	GGAATGGATGGCTACCGTGG	CATGCCACCCATGCTCGAAT	27
EEC[a]	*Chga*	TTCCATGCAGGCTACAAAG	GTCTTTCCATCTCCATCCAC	28
Goblet cell	*Muc2*	ATGCCCACCTCCTCAAAGAC	GTAGTTTCCGTTGGAACAGTGAA	29
Enterocyte	*Villin*	CACTCACACAAGACCTGCTCAAG	ACTGCTTGGCTTTGATGAAGTTCA	
TA cell[b]	*Ki67*	ATCATTGACCGCTCCTTTAGGT	GCTCGCCTTGATGGTTCCT	27
Normalization	*Gapdh*	AGGTCGGTGTGAACGGATTTG	TGTAGACCATGTAGTTGAGGTCA	30

[a] EEC = enteroendocrine cell. [b] TA = transit amplifying.

from 500 ng of RNA using the iScript™ cDNA synthesis kit (BioRad) according to manufacturer's instructions. The following thermal cycling conditions were used: 5 min at 25 °C, 20 min at 46 °C, and 1 min at 95 °C. Primer sequences were obtained at the online PrimerBank database and/or from literature (Table 1). qPCR was performed with a CFX384 thermal cycler (BioRad) using the SensiMix SYBR No-ROX kit (Bioline, Alphen aan de Rijn, the Netherlands). The housekeeping gene *Gapdh* was used for normalization.

To compare the relative gene expression of epithelial cell markers in the enteroids and mice, microarray data obtained from mucosal scrapings from jejunal tissue (generated from 3 male C57BL/6 mice) was used.[31]

2.10. Statistical data analysis

Cytotoxicity (LDH), cell viability (WST-1), and gene expression between enteroids and *in vivo* data were analyzed by analysis of variance (ANOVA) using GraphPad Prism 9.3.1 (Boston, MA, USA). Significant differences ($p \leq 0.05$) were compared with the negative control using Dunnett's *post hoc* comparisons. Differences in gene expression of intestinal cell markers between passages and between apical-in and apical-out enteroids was analyzed by multiple unpaired *t*-tests with Welch's correction, respectively.

3. Results

3.1. Glabridin, licochalcone A, and glycycoumarin show a dose-dependent cytotoxicity in mouse apical-in enteroids

Before determining the cytotoxicity of prenylated phenolics in apical-out enteroids, we assessed the cytotoxicity of glab, licoA, and glycy in apical-in enteroids after 4 h and 24 h of exposure. This apical-in enteroid model is currently the state-of-the-art model. However, here the basolateral side is exposed to the experimental agents. Cytotoxicity was determined by the release of LDH (Fig. 2). Glab, licoA, and glycy displayed a dose-dependent increase in cytotoxicity after 4 h and 24 h of exposure (Fig. 2A). Glab did not exhibit any significant cytotoxicity up to 75 μg mL^{-1} (231 μM) after 4 h and up to 25 μg mL^{-1} (77 μM) after 24 h, compared to the negative control. Significant cytotoxicity (28% cytotoxicity) for glab was seen at 100 μg mL^{-1} (309 μM, $p < 0.0001$) and at 37.5 μg mL^{-1} (36% cytotoxicity) (116 μM, $p < 0.0001$) after 4 h and 24 h stimulation, respectively. After 4 h exposure, licoA showed 32% cytotoxicity at 250 μg mL^{-1} (740 μM, $p = 0.01$), while for glab cytotoxicity was observed at a lower concentration (100 μg mL^{-1}). After 24 h licoA showed comparable cytotoxicity as glab, with 56% cytotoxicity at 37.5 μg mL^{-1} (111 μM, $p < 0.0001$). Lastly, glycy seemed less cytotoxic compared to aforementioned compounds, as no significant cytotoxicity was observed up to 250 μg mL^{-1} (679 μM) after 4 h, and up to 50 μg mL^{-1} (136 μM) after 24 h. Significant cytotoxicity after 24 h glycy exposure was observed at 62.5 μg mL^{-1} (170 μM, $p < 0.0001$).

Half-maximal cytotoxic concentrations (IC_{50}) of glab, licoA, and glycy after 24 h incubation were calculated (Fig. 2B), and were established at 49 μg mL^{-1} (151 μM) for glab, 37 μg mL^{-1} (109 μM) for licoA, and 60 μg mL^{-1} (163 μM) for glycy. Moreover, glycy cytotoxicity was observed with a distinct off–on effect, whereas glab and licoA showed a more gradual dose–response effect, as was shown by the steepness of the regression slopes (Fig. 2B).

Additionally, effects on cell viability (by the Live–Dead cell viability assay) after 24 h of incubation with glab, licoA, and glycy on apical-in mouse enteroids were assessed by staining live and dead cells with calcein AM (green) and propidium iodide (red), respectively (Fig. 2C). In agreement with our LDH assay, non-cytotoxic concentrations of 25 μg mL^{-1} (74 μM) licoA and 50 μg mL^{-1} (136 μM) glycy did not visually show cytotoxicity. Also incubation with 37.5 μg mL^{-1} (116 μM) of glab did not visually increase the amount of dead cells, even though this concentration did show significant cytotoxicity (37% cytotoxicity compared to the negative control, $p < 0.001$, Fig. 2A). Toxic concentrations of glab (75 μg mL^{-1}, [116 μM]), licoA (37.5 μg mL^{-1} [111 μM]), and glycy (75 μg mL^{-1} [204 μM]) resulted in brightly red colored, irregularly shaped, enteroids, indicating non-viable or dead enteroids.

In order to validate the robustness of the established general cytotoxicity model, cytotoxicity of glab in apical-in enteroids from different passages was assessed (Fig. B2, ESI†). Passage number hardly influenced the assessed cytotoxicity of glab in apical-in enteroids, with established IC_{50}'s of 49 ± 0.6 μg mL^{-1} (151 ± 1.0 μM) in enteroids with high passage

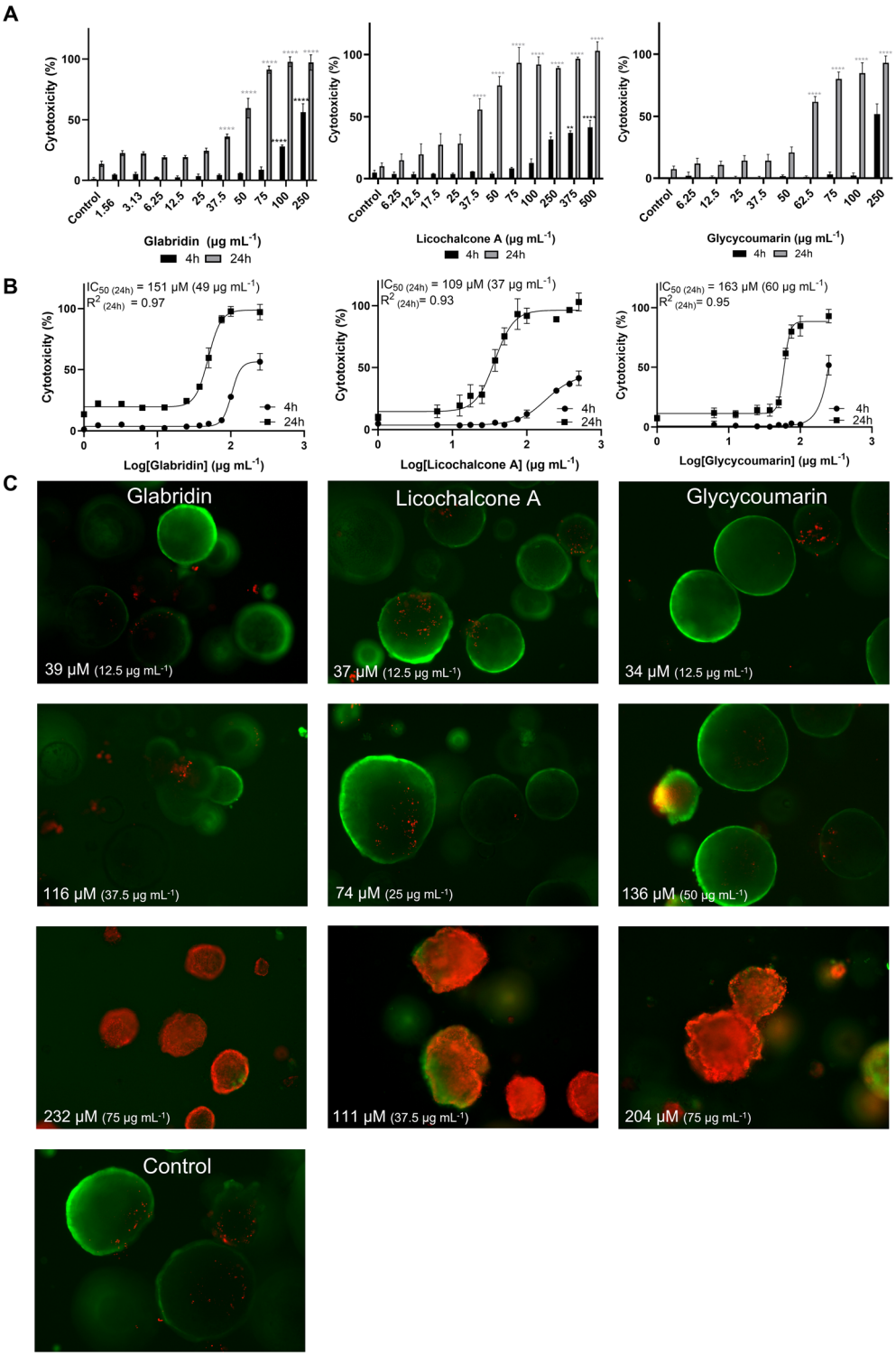

Fig. 2 Cytotoxicity of mouse apical-in jejunal enteroids after glabridin, licochalcone A, and glycycoumarin exposure. (A) Cytotoxicity of glabridin, licochalcone A, and glycycoumarin after 4 h and 24 h stimulation in mouse apical-in enteroids by LDH (in μg mL^{-1}), (B) their half-maximal cytotoxic concentrations (IC_{50}) determined by LDH after 24 h incubation (in μM), and (C) visual assessment of cell viability by the Live–Dead cell viability assay after 24 h incubation. Live cells are stained green (calcein AM) and dead cells are stained red (propidium iodide). For the statistics, data are compared to the control and expressed as the mean ± SEM of three biological replicates, measured in duplicate. *$p < 0.05$, **$p < 0.01$, ***$p < 0.001$, and ****$p < 0.0001$.

number (>30) and 42 ± 0.7 μg mL^{-1} (129 ± 1.3 μM) in enteroids with low passage number (<13).

3.2. The apical microvilli brush border is faced outwards in mouse apical-out enteroids

The polarity of mouse enteroids was reversed according to the protocol of Co *et al.* for human enteroids.[21,22] In brief, we removed the ECM, thereby disrupting interactions between gel proteins with basolateral β1 integrin receptors in the enteroids. This triggered a coordinated movement of the epithelium, resulting in eversion of enteroid polarity without alterations to individual cells.[21,22] We successfully produced apical-out mouse enteroids, as shown by staining F-actin in the cytoskeleton (Fig. 3). During polarity reversal, the microvilli brush border moved from the inside of the apical-in enteroid (Fig. 3A) towards the outside of the apical-out enteroid (Fig. 3B). Also, suspended apical-out enteroids visually lacked a lumen, which was present in apical-in enteroids (see dark inner circle, Fig. 3A, upper right panel). Besides a thick F-actin layer on the luminal side of apical-in enteroids (Fig. 3A, upper right panel), a thin F-actin layer on the basolateral side was seen as well.[32] By generating this apical-out model enteroids can be easily exposed from their apical side.

3.3. Mucus surrounds the apical microvilli brush border in apical-out enteroids

After the polarity of mouse apical-in enteroids was reversed, we stained the fucose units in the mucus layer in apical-out enteroids with *Ulex europaeus* agglutinin I rhodamine, which binds to mucosal glycoproteins containing α-linked fucose residues (Fig. 4). Fucosylation is ubiquitous in the intestinal epithelium in mice.[33,34] From Fig. 4 it can be seen that the apical-out mouse enteroids exhibit a fucose containing mucus layer surrounding the apical brush-border (Fig. 4A). In apical-in enteroids, however, this fucose containing mucus layer is located at the apical brush-border surrounding the lumen (Fig. 4B). Interestingly, at sites where F-actin in the cytoskeleton was not stained in the apical-out enteroid (Fig. 4A, white arrows), the fucose containing mucus was absent, indicating that the enteroid did not always completely reverse polarity.

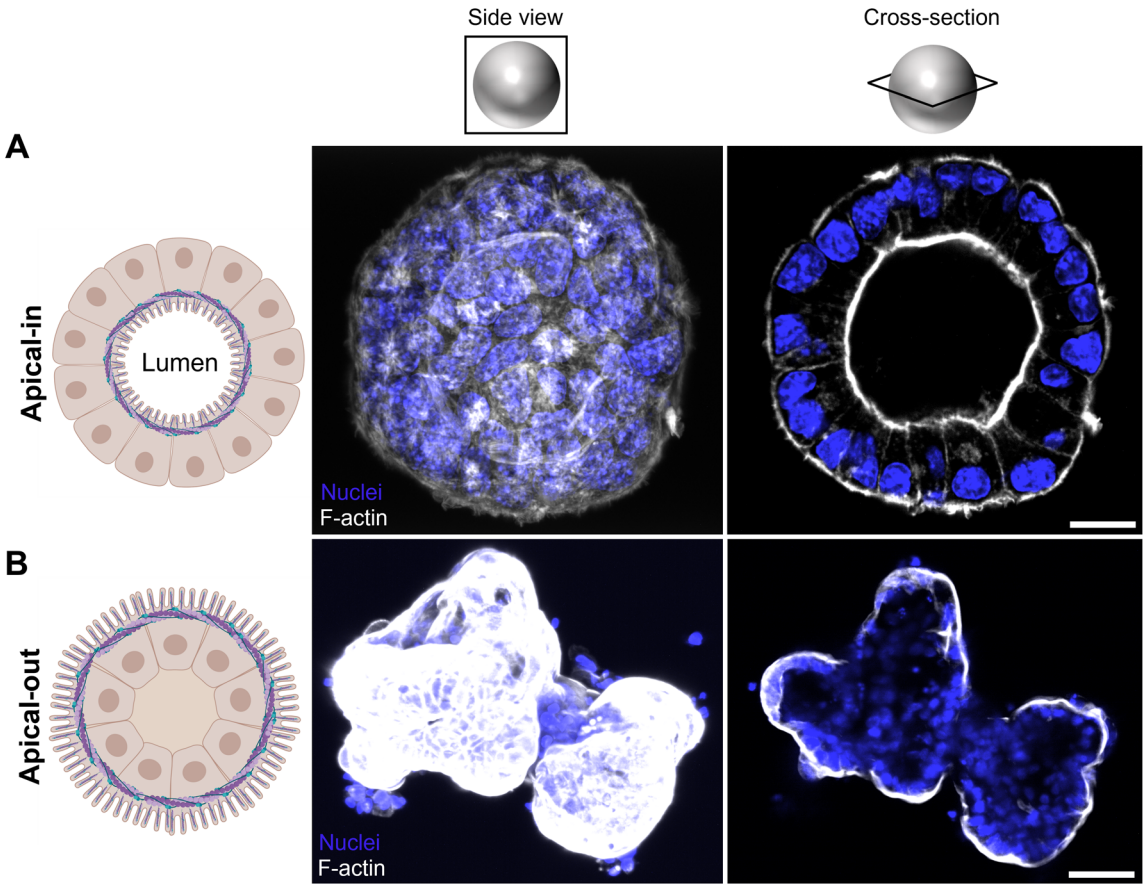

Fig. 3 Polarity reversal in mouse jejunal enteroids shown by confocal imaging. Panels (A) show apical-in enteroids schematically (left; actin cytoskeleton in purple) and confocal images of suspended mouse enteroids with an apical-in polarity (middle and right) and panels (B) show apical-out enteroids schematically (left; actin cytoskeleton in purple) and confocal images of mouse enteroids with an apical-out polarity (middle and right). Nuclei were visualized with DAPI (blue) and the actin cytoskeleton in the microvilli brush border was stained with ActinRed™ 555 (white). Scale bars in panels (A) and (B) are 10 μm and 30 μm, respectively. Illustrations in (A) and (B) were created with BioRender.com.

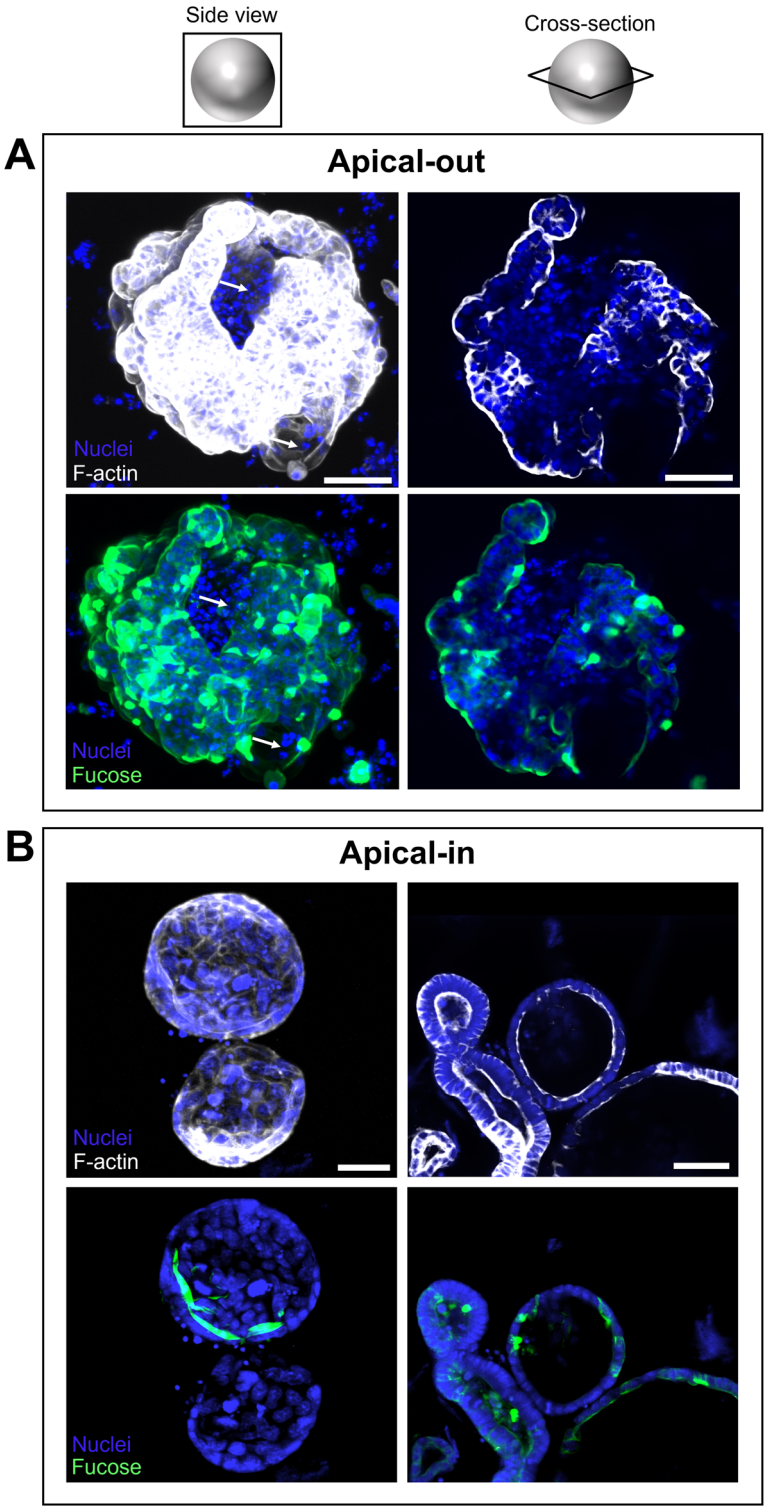

Fig. 4 Fucose staining of mucosal glycoproteins in apical-out and apical-in mouse jejunal enteroids. Confocal side views and cross-sections of apical-out (A) and apical-in (B) mouse enteroids stained for actin (shown in white) and for fucose units attached to mucus (shown in green). The white arrows in panels A show parts of the enteroids that have an apical-in polarity and are not flipped. Nuclei were visualized with DAPI (shown in blue), the actin cytoskeleton in the microvilli brush border was stained with AlexaFluor™ 660 Phallaoidin (white), and fucose units in the mucus layer was stained with *Ulex Europaeus* Agglutinin I Rhodamine (fucose) (shown in green). Scale bars are 30 μm.

3.4. Gene expression of intestinal epithelial cell markers in apical-out enteroids reflects *in vivo* gene expression better than apical-in enteroids

To establish whether the generated apical-out enteroids retained their specific gene expression profile, we compared the gene expression of epithelial cell markers (stem cells, transit amplifying cells, goblet cells, enteroendocrine cells, Paneth cells, and absorptive enterocytes) from both enteroid models, and compared this to the gene expression of mucosal jejunal scrapings from C57BL/6 mice (Fig. 5).[31] Apical-out enteroids showed a reduction of *lgr5* (stem cells) and *ki67* (transit amplifying cells) expression compared to apical-in enteroids (Fig. 5A, $p < 0.05$), suggesting a shift to differentiation when changing the enteroids' polarity. Apical-out enteroids also showed downregulation of *chga* and *lyz* expression, suggesting the presence of fewer enteroendocrine and Paneth cells compared to apical-in enteroids. Markers for goblet cells (*muc2*) and enterocytes (*villin*) were equivalent between both enteroid models. It should be noted that apical-in and apical-out enteroids were grown in mIC and hIC medium, respectively, and thus a medium effect could possibly also affect the observed differences in gene expression: based on the gene expression of epithelial markers in apical-in enteroids grown in hIC, it was shown that medium also affected the gene expression of epithelial cell markers, besides enteroid polarity (*e.g. chga* expression, Fig. C3A, ESI†).

Based on the ratio in gene expression between epithelial markers (*lgr5*, *ki67*, *muc2*, *chga*, and *lyz*) and *villin*, it seemed that apical-out enteroids show a better resemblance to *in vivo* jejunal tissue compared to apical-in enteroids grown in mIC and hIC (Fig. 5B and Fig. C3B, ESI†): the relative gene expression of epithelial markers (with the exception of *lyz*) in apical-out enteroids and *in vivo* tissue was comparable ($p > 0.05$), whereas expression of *lgr5*, *ki67*, *chga*, and *lyz* in apical-in enteroids was significantly different compared to *in vivo* tissue (Fig. 5B). Lastly, we compared the gene expression of all epithelial markers in enteroids with a low (passages < 15) and high (passages > 15) passage number (Fig. C3A, ESI†). Passage number did not affect gene expression of epithelial cell markers in apical-in and apical-out enteroids.

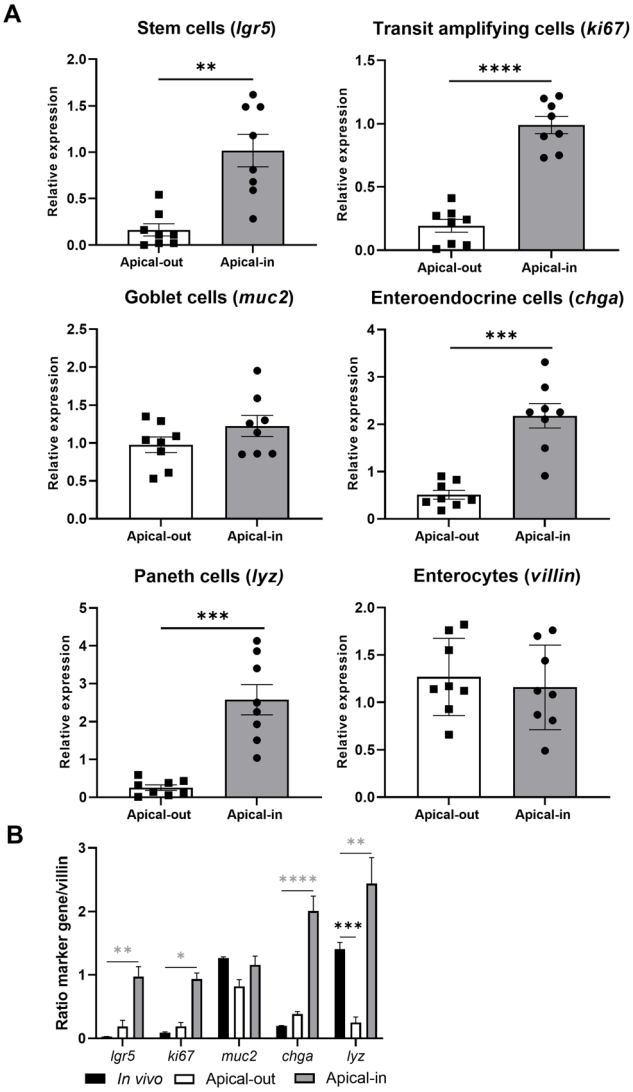

Fig. 5 Gene expression of epithelial cell markers in apical-out and apical-in enteroids. Panel (A) shows qRT-PCR gene expression analysis of epithelial cell markers for stem cells (*lgr5*), transit amplifying cells (*ki67*), goblet cells (*muc2*), enteroendocrine cells (*chga*), Paneth cells (*lyz*), and enterocytes (*villin*) in apical-out and apical-in enteroids, grown in human (hIC) and mouse growth medium (mIC), respectively. Gene expression was normalized to *gapdh* housekeeping gene. Panel (B) shows the ratio between gene expression of epithelial markers (*lgr5*, *ki67*, *muc2*, *chga*, *lyz*) compared to *villin* gene expression in (1) jejunal scrapings from C57BL/6 mice,[31] (2) apical-out (relative towards *gapdh*; grown in hIC), and (3) apical-in enteroids (relative towards *gapdh* grown in mIC). Data are expressed as the mean ± SEM of eight biological replicates, measured in duplicate. *In vivo* data from (B) were measured in three biological replicates. *$p < 0.05$, **$p < 0.01$, ***$p < 0.001$, and ****$p < 0.0001$.

3.5. Glabridin shows lower cytotoxicity with apical-out mouse enteroids than with apical-in mouse enteroids

After establishing apical-out enteroids, we determined intestinal *in vitro* cytotoxicity of the promising antibacterial glab by measuring the release of LDH, and determining the effect of glab exposure on the enteroids' viability by measuring mitochondrial dehydrogenase by WST-1. Cytotoxicity and cell viability results are shown in Fig. 6.

Apical-out enteroids seemed to better tolerate glab exposure than apical-in enteroids, as significant cytotoxicity in apical-out enteroids was observed at 500 μg mL^{-1} glab (1543 μM) with 36% ($p = 0.005$) and 67% cytotoxicity ($p < 0.0001$) after 4 h and 8 h exposure, respectively (Fig. 6A), whereas significant cytotoxicity in apical-in enteroids was observed at 100 μg mL^{-1} (309 μM) after 4 h exposure (Fig. 2A). Cytotoxic IC_{50} values were not established, as we did not observe a 100% cytotoxic response after 4 h and 8 h glab incubation at the highest concentration tested (Fig. 6B). Cell viability (or mitochondrial activity, as measured by WST-1) was affected at lower concentrations than where cytotoxicity was observed after 4 h

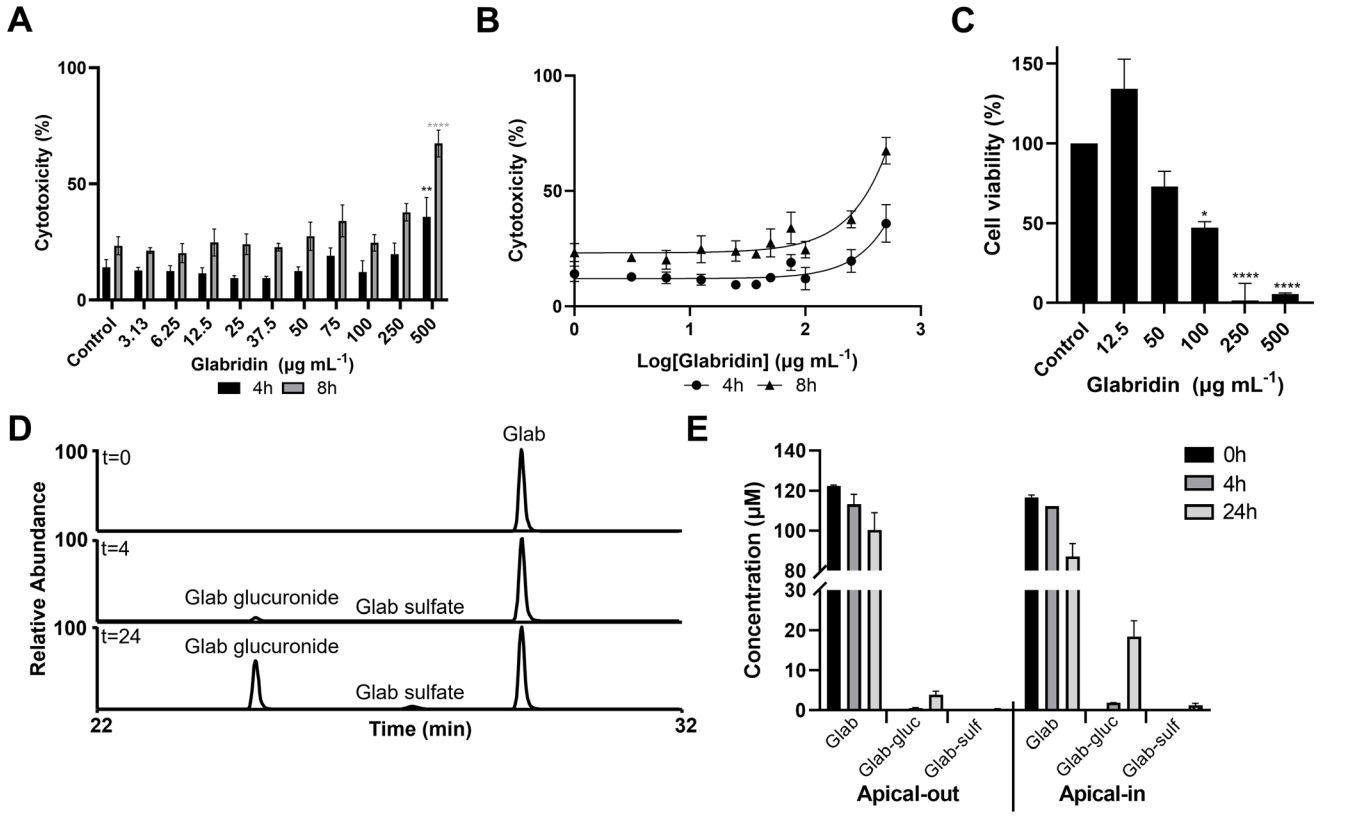

Fig. 6 Cytotoxicity, cell viability, and biotransformation of glabridin (glab) in mouse apical-out jejunal enteroids. (A) Enteroid cytotoxicity (by LDH) after 4 h and 8 h glabridin stimulation in μg mL^{-1}, (B) non-linear regression analysis of enteroid cytotoxicity (by LDH) after 4 h and 8 h glabridin stimulation in log μg mL^{-1}, (C) cell viability of apical-out enteroids after 4 h glabridin exposure in μg mL^{-1}, (D) representative RP-UHPLC-MS chromatograms of biotransformation of glabridin between 22 and 32 min in negative ionization mode extracted ion chromatograms at *m/z* 323 (glab), *m/z* 403 (glab-sulfate), and *m/z* 499 (glab-glucuronide) at *t* = 0 h (top), *t* = 4 h (middle), and *t* = 24 h (bottom), and (E) comparison of biotransformation of glabridin in apical-out and apical-in enteroids over time. The highest tested concentration of glab was 500 μg mL^{-1} (of note, higher concentrations of glab were not soluble in organoid medium). Glab-gluc = glabridin-glucuronide and glab-sulf = glabridin-sulfate. Data are expressed as the mean ± SEM of three biological replicates, measured in duplicate, except for panel C, where 12.5 μg mL^{-1}: *n* = 2, measured in duplicate, and 500 μg mL^{-1}: *n* = 1, measured in duplicate. **p* < 0.05, ***p* < 0.01, ****p* < 0.001, and *****p* < 0.0001.

exposure to glab, and a clear dose–response relationship between glab concentration and cell viability was seen (Fig. 6C). Up to 50 μg mL^{-1} (154 μM) there was no significant reduction on enteroid viability, whereas at 100 μg mL^{-1} (309 μM) glab decreased the cell viability to 47% (p = 0.001) compared to the negative control (set at 100% viability).

The enteroids were exposed to glab only for 4 h and 8 h, as we noticed after 24 h a high intrinsic LDH release in the negative control (Fig. D4A, ESI†), which was hypothesized to be (partly) caused by shedding of dead intestinal cells from the villus tip to the intestinal lumen (the small intestinal epithelium turnover in mice takes about 1–2.5 days[35]). Washing the apical-out enteroids decreased the high intrinsic LDH concentrations in the negative control, and thus the measured cytotoxicity (Fig. D4B, ESI†). Nevertheless, the cell viability after 24 h was greatly reduced compared to the control (at 0 h of incubation), see Fig. D4C, ESI.†

Lastly, we determined the biotransformation of glab (at non-toxic concentrations) in both apical-out (section 3.4) and apical-in (section 3.1) enteroids, *i.a.* in order to assess whether the determined cytotoxicities were caused by glab itself and/or by its possible metabolites. Identification of metabolites was based on comparison of spectroscopic and spectrometric data with those from literature.[36] Annotations of all metabolites are shown in Table E1 (ESI†). Both apical-out and apical-in enteroids were able to transform glab into glucuronide and sulfate metabolites, although apical-out enteroids transformed lower amounts compared to the conventional apical-in enteroids (Fig. 6D and E). After 4 h of glab incubation, glab-glucuronide was detected in both apical-out and apical-in enteroids, at concentrations of 0.6 μM and 1.9 μM, respectively. Glucuronides increased further to 3.9 μM in apical-out and to 18.4 μM in apical-in enteroids after 24 h glab incubation (notably the apical-out enteroids were shown to have a reduced cell viability at 24 h [Fig. D4C, ESI†]). Glab-sulfate could only be quantified after 24 h of glab incubation, at concentrations of 0.3 μM and 1.3 μM in apical-out and apical-in enteroids, respectively. Biotransformation of licoA and glycy was only determined in apical-in enteroids, where the main products formed were also phase II metabolites, glucuronides and sulfates (Fig. F5, ESI†).

Besides phase II metabolites, we tentatively identified phase I metabolites of licoA and glycy in apical-in enteroids (Table E1 and Fig. F5, ESI†). LicoA was, amongst others, metabolized to saturated-licoA (possibly by hydrogenation of the double bond between the A-ring and B-ring, Fig. 1), which was further glucuronidated to saturated-licoA-glucuronide. For glycy, *i.a.* the prenyl chain was metabolized by hydroxylation.[37]

4. Discussion

4.1. Mouse apical-out enteroids offer a relevant gastrointestinal model, well-suited for conducting cytotoxicity and cell viability screening

We successfully developed a mouse apical-out enteroid model that provides several advantages over the currently most used apical-in model. The model is suitable to study the *in vitro* bioactivity and toxicity of compounds that may be present in the intestine, such as nutrients, non-nutrient bioactive food-components, drugs, and metabolites formed in the intestine. Apical-out enteroids can be suspended in culture medium and do not require embedding in ECM. Because their apical surface is faced to the outside and not towards the lumen, these enteroids better mimic the *in vivo* situation and can easily be exposed to test compounds, without the need of micro-injection. Furthermore, we demonstrated that mucus is formed outwards at the luminal/apical side, as was visualized by the fucose containing mucus layer, representative of the proximal small intestine.[38] Moreover, we showed that the epithelial cell marker profile in apical-out enteroids were a better mimic of their *in vivo* counterpart compared to apical-in enteroids. The enteroids also demonstrated phase II biotransformation capacity. As was demonstrated by Co *et al.* for human apical-out enteroids, apical-out enteroids have shown to recapitulate properties and functions of the native intestinal epithelium, including barrier function, absorptive, and secretory properties.[21,22]

We showed that apical-out enteroids were less susceptible towards glab compared to the conventional apical-in enteroids, as cytotoxicity (as measured by LDH) after 4 h glab stimulation was 5 times lower in apical-out than in apical-in enteroids. This reduced susceptibility can possibly be explained by the hydrophilic mucus layer (consisting of *O*-glycans such as *N*-acetylglucosamine, galactose, and fucose units[25]) surrounding the apical-out enteroids. We hypothesize that the hydrophobic properties of glab impede its diffusion through the hydrophilic mucus layer, thereby restricting its exposure to the epithelial cells. Apical-out enteroids were found suitable for cytotoxicity testing at least up to 8 h incubation, as we did observe decreased mitochondrial activity in enteroids after 24 h. Shorter incubation times are more representative of the *in vivo* situation since the small intestinal transit time in mice is approximately 90 min.[39] Besides cytotoxicity, we found reduced mitochondrial activity after glab exposure at lower concentrations as measured by LDH.

Next to determining intestinal cytotoxicity in apical-out enteroids, we assessed the cytotoxicity in the conventional apical-in model, which is still a more commonly used model in biomedical research.[18] With this model, experimental agents are added to the basolateral surface of the enteroids, which is a different situation from that which occurs *in vivo* upon exposure to substances in the lumen. Therefore, such a set-up is less suitable for evaluation of intestinal toxicity of drugs and other bioactives. However, our comparison of the prenylated phenolics in apical-in enteroids gives a good indication of cytotoxicity in healthy tissue. Our results demonstrate that 4 h basolateral exposure to glab seemed to be most toxic, followed by exposure to licoA and glycy, respectively. After 24 h basolateral exposure, licoA and glab showed higher cytotoxicity than glycy. In literature, effects on cytotoxicity and/or cell viability of glab, licoA, and glycy in mice are described for mouse skin, fibroblast, and liver derived cell lines, in which reported cytotoxicities occurred at lower concentrations (~30 μM) than those observed in our study.[40–42] In cell lines, it has been shown that the cytotoxic mode of action of licoA, glycy and structural similar compounds of glab (glabrene and 4′-*O*-methylglabridin), was related to changes in cell cycle signaling pathways, ultimately leading to apoptotic cell death *via* different mechanisms.[43–47] We observed that apical-in enteroids exposed to cytotoxic concentrations of glab, licoA, and glycy showed morphological changes compared to non-cytotoxic concentrations, which could possibly suggest membrane permeabilization and/or membrane disruption. Antibacterial mode of action of prenylated phenolics has been implicated with the interaction, permeabilization, and/or disruption of the bacterial membrane.[48] In order to determine if prenylated phenolics interact with the enteroids' cell membranes, further research regarding *e.g.* barrier integrity needs to be done.[21]

4.2. Mouse enteroids are able to transform prenylated phenolics into other metabolites

In this study we demonstrate that apical-out and apical-in enteroids are able to transform prenylated phenolics into their glucuronides and sulfates. These phase II biotransformation reactions are catalyzed by UDP-glucuronosyltransferases (UGTs) located in the endoplasmic reticulum and by cytosolic sulfotransferases (SULT), respectively and are known to take place in enterocytes and the liver, rendering the compounds more hydrophilic.[49–51] Besides phase II biotransformation, we also observed some phase I biotransformation reaction products derived from licoA and glycy, such as saturated-licoA (by hydrogenation of the double bond between the A and the B-ring, Fig. 1) and glycy with hydroxylation on the prenyl chain.[37]

Compared to apical-out enteroids, apical-in enteroids showed a higher capacity to metabolize glab. This could be explained by the mucus layer surrounding the apical-out enteroids, which impedes the entrance of glab into the enterocytes. Alternatively, glab could be subjected to polarized transport (apical to basolateral and *vice versa*), as was shown by Cao and co-workers.[26] Incubation for 4 h showed little biotransform-

ation of glab, suggesting that the effects on cytotoxicity and cell viability are likely due to the parent compound and not to its metabolites. Overall, these results demonstrate that enteroids are useful for determining intestinal biotransformation, in contrast to *e.g.* Caco-2 cells, in which *i.a.* CYP enzymes are missing.[18,52]

4.3. Glabridin, licochalcone A, and glycycoumarin do not exhibit cytotoxicity in enteroids at concentrations equivalent to their minimum inhibitory concentration (MIC) values against Gram-positive bacteria

Lastly, we compiled and compared all measured cytotoxicity data (measured with LDH) and cell viability data (measured with WST-1) after 4 h exposure to prenylated phenolics in apical-in and apical-out enteroids. This was compared with our previously obtained cytotoxicity data in Caco-2 cells and our reported MICs against a variety of Gram positive bacteria.[1] A schematic summary of the highest non-toxic concentrations and highest concentrations where cell viability was not impaired is shown in Fig. 7.

The highest non-toxic concentrations for glab, licoA, and glycy in apical-in and apical-out enteroids were higher than their MICs (between 9.3–77 μM) against various Gram positive bacteria (*Lactobacillus buchneri*, *Streptococcus mutans*, and *Staphylococcus aureus*), as tested in van Dinteren *et al.*[1] However, against Gram negative bacteria (*Escherichia coli*) and yeasts (*Zygosaccharomyces parabailli* and *Yarrowia lipolytica*), cytotoxicity was observed at antibacterial concentrations (MICs between [271–309] μM (ref. 1)). Both enteroid models were more resilient than Caco-2 cells, where cytotoxicity and reduced cell viability was observed at concentrations equivalent to the MICs. However, it should be noted that direct comparison of concentrations between various model systems with different experimental conditions should be approached with caution, as it only provides indicative information. When comparing our previously reported cytotoxicities in human Caco-2 cells of glab, licoA, and glycy with published cytotoxicities in mouse cell lines, cytotoxicity in Caco-2 cells seems to be at roughly twice the concentration (~70–140 μM (ref. 1)) compared to those in different mouse cell lines (IC_{50}'s of ~ 30 μM (ref. 40 and 42)).

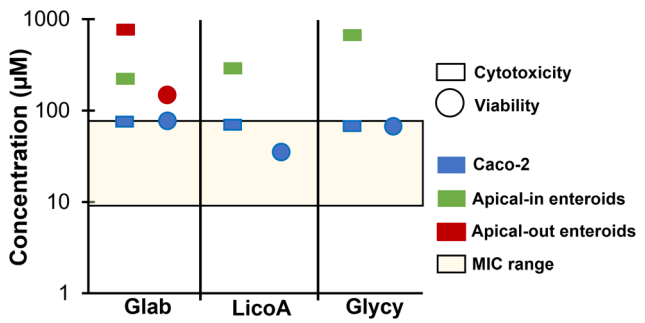

Fig. 7 Comparisons of cytotoxicity and viability of glabridin (glab), licochalcone A (licoA), and glycycoumarin (glycy) for different models. Schematic summary of highest non-toxic concentrations (measured with the LDH assay, shown in squares) and non-reducing cell viabilities (measured with the WST-1 assay, shown in circles) of glab, licoA, and glycy with their reported minimum inhibitory concentrations (MICs) against a variety of Gram positive bacteria (shown as a range in the yellow shaded box)[1] in human colon cancer (Caco-2) cells (shown in blue),[1] apical-in mouse enteroids (shown in green), and apical-out mouse enteroids (shown in red).

5. Conclusion

We successfully developed a mouse apical-out enteroid model to evaluate the effects of prenylated phenolics on cytotoxicity and cell viability. Compared to conventional apical-in enteroids, the novel model represents the small intestine relatively well, as shown by the comparison of the gene expression of epithelial cell markers with those from *in vivo* jejunal tissue. The newly developed model allowed us to assess cytotoxicity and cell viability of glab, which neither showed cytotoxicity nor negative effects on the cells' metabolic activity at concentrations where it is effective against Gram positive bacteria. Apical-out enteroids were more robust towards glab than the conventional apical-in enteroids and exhibited less functional phase II biotransformation capacity, possibly due to the hydrophilic mucus layer surrounding them. Also for licoA and glycy no general cytotoxicity in small intestinal apical-in enteroids at their MICs against Gram positive bacteria was observed. Our results indicate that the potential antimicrobials from licorice roots do not show *in vitro* cytotoxicity in mouse enteroids at their MICs against Gram positive bacteria. A logical next step is to verify these findings in human enteroids.

Author contributions

Sarah van Dinteren: Conceptualization, methodology, investigation, visualization, writing – original draft, preparation. Carla Araya-Cloutier: Conceptualization, methodology, writing – review & editing, supervision. Edyta Robaczewska: Investigation. Mellody den Otter: Investigation. Jean-Paul Vincken: Writing – review & editing, supervision. Renger Witkamp: Conceptualization, writing – review & editing. Jocelijn Meijerink: Conceptualization, methodology, writing – review & editing, supervision.

Conflicts of interest

The authors declare that they have no known competing conflict of interest or personal relationships that could have appeared to influence the work reported in this paper.

Acknowledgements

The authors would like to thank Rianne Jansen for her input on the microarray data of intestinal cell markers from *in vivo* jejunal C57BL/6 scrapings and Josep Rubert for his input on

fluorescence staining of enteroids. This work was supported by Topconsortium voor Kennis en Innovatie (TKI, grant number TKI-AF-18124). Private partners did not have any influence on the scientific content.

References

1 S. van Dinteren, J. Meijerink, R. Witkamp, B. van Ieperen, J.-P. Vincken and C. Araya-Cloutier, Valorisation of liquorice (*Glycyrrhiza*) roots: antimicrobial activity and cytotoxicity of prenylated (iso)flavonoids and chalcones from liquorice spent (*G. glabra*, *G. inflata*, and *G. uralensis*), *Food Funct.*, 2022, **13**, 12105–12120.

2 S.-Q. Fang, Q.-Y. Qu, Y. F. Zheng, H. H. Zhong, C. X. Shan, F. Wang, C. Y. Li and G. P. Peng, Structural characterization and identification of flavonoid aglycones in three Glycyrrhiza species by liquid chromatography with photodiode array detection and quadrupole time-of-flight mass spectrometry, *J. Sep. Sci.*, 2016, **39**, 2068–2078.

3 W. Song, X. Qiao, K. Chen, Y. Wang, S. Ji, J. Feng, K. Li, Y. Lin and M. Ye, Biosynthesis-Based Quantitative Analysis of 151 Secondary Metabolites of Licorice To Differentiate Medicinal *Glycyrrhiza*, Species and Their Hybrids, *Anal. Chem.*, 2017, **89**, 3146–3153.

4 S. van Dinteren, C. Araya-Cloutier, W. J. C. de Bruijn and J.-P. Vincken, A targeted prenylation analysis by a combination of IT-MS and HR-MS: identification of prenyl number, configuration, and position in different subclasses of (iso)flavonoids, *Anal. Chim. Acta*, 2021, **1180**, 338874.

5 N. C. Veitch, Isoflavonoids of the Leguminosae, *Nat. Prod. Rep.*, 2013, **30**, 988–1027.

6 M. Carocho, M. F. Barreiro, P. Morales and I. C. F. R. Ferreira, Adding Molecules to Food, Pros and Cons: A Review on Synthetic and Natural Food Additives, *Compr. Rev. Food Sci. Food Saf.*, 2014, **13**, 377–399.

7 C. L. Ventola, The antibiotic resistance crisis: part 1: causes and threats, *Pharm. Ther.*, 2015, **40**, 277–283.

8 C. Araya-Cloutier, J.-P. Vincken, R. van Ederen, H. M. W. den Besten and H. Gruppen, Rapid membrane permeabilization of *Listeria monocytogenes* and *Escherichia coli*, induced by antibacterial prenylated phenolic compounds from legumes, *Food Chem.*, 2018, **240**, 147–155.

9 B. Botta, A. Vitali, P. Menendez, D. Misiti and G. D. Monache, Prenylated flavonoids: Pharmacology and biotechnology, *Curr. Med. Chem.*, 2005, **12**, 713–739.

10 A. Bartmańska, T. Tronina, J. Popłoński, M. Milczarek, B. Filip-Psurska and J. Wietrzyk, Highly Cancer Selective Antiproliferative Activity of Natural Prenylated Flavonoids, *Molecules*, 2018, **23**, 2922.

11 C. Dorn, T. S. Weiss, J. Heilmann and C. Hellerbrand, Xanthohumol, a prenylated chalcone derived from hops, inhibits proliferation, migration and interleukin-8 expression of hepatocellular carcinoma cells, *Int. J. Oncol.*, 2010, **36**, 435–441.

12 C.-H. Jiang, T.-L. Sun, D.-X. Xiang, S.-S. Wei and W.-Q. Li, Anticancer Activity and Mechanism of Xanthohumol: A Prenylated Flavonoid From Hops (*Humulus lupulus*, L.), *Front. Pharmacol.*, 2018, **9**, 530.

13 L. Molčanová, D. Janošíková, S. Dall'Acqua and K. Šmejkal, C-prenylated flavonoids with potential cytotoxic activity against solid tumor cell lines, *Phytochem. Rev.*, 2019, **18**, 1051–1100.

14 F. Li, S. Awale, Y. Tezuka and S. Kadota, Cytotoxic Constituents of Propolis from Myanmar and Their Structure-Activity Relationship, *Biol. Pharm. Bull.*, 2009, **32**, 2075–2078.

15 S. Lechuga, M. B. Braga-Neto, N. G. Naydenov, F. Rieder and A. I. Ivanov, Understanding disruption of the gut barrier during inflammation: Should we abandon traditional epithelial cell lines and switch to intestinal organoids?, *Front. Immunol.*, 2023, **14**, 640.

16 D. Ahmed, P. W. Eide, I. A. Eilertsen, S. A. Danielsen, M. Eknaes, M. Hektoen, G. E. Lind and R. A. Lothe, Epigenetic and genetic features of 24 colon cancer cell lines, *Oncogenesis*, 2013, **2**, e71.

17 T. R. Chen, D. Drabkowski, R. J. Hay, M. Macy and W. Peterson, Widr Is a Derivative of Another Colon Adenocarcinoma Cell-Line, HT-29, *Cancer Genet. Cytogenet.*, 1987, **27**, 125–134.

18 Y. Takahashi, M. Noguchi, Y. Inoue, S. Sato, M. Shimizu, H. Kojima, T. Okabe, H. Kiyono, Y. Yamauchi and R. Sato, Organoid-derived intestinal epithelial cells are a suitable model for preclinical toxicology and pharmacokinetic studies, *iScience*, 2022, **25**, 104542.

19 T. Sato, R. G. Vries, H. J. Snippert, M. van de Wetering, N. Barker, D. E. Stange, J. H. van Es, A. Abo, P. Kujala, P. J. Peters and H. Clevers, Single Lgr5 stem cells build crypt-villus structures *in vitro* without a mesenchymal niche, *Nature*, 2009, **459**, 262–265.

20 T. Sato and H. Clevers, Growing Self-Organizing Mini-Guts from a Single Intestinal Stem Cell: Mechanism and Applications, *Science*, 2013, **340**, 1190–1194.

21 J. Y. Co, M. Margalef-Catala, D. M. Monack and M. R. Amieva, Controlling the polarity of human gastrointestinal organoids to investigate epithelial biology and infectious diseases, *Nat. Protoc.*, 2021, **16**, 5171–5192.

22 J. Y. Co, M. Margalef-Catala, X. Li, A. T. Mah, C. J. Kuo, D. M. Monack and M. R. Amieva, Controlling Epithelial Polarity: A Human Enteroid Model for Host-Pathogen Interactions, *Cell Rep.*, 2019, **26**, 2509–2520.

23 D. Zhang, X. Zhou, W. Zhou, S. W. Cui and S. Nie, Intestinal organoids: A thriving and powerful tool for investigating dietary nutrients-intestinal homeostasis axis, *Food Res. Int.*, 2023, **172**, 113109.

24 A. MacAdam, The effect of gastro-intestinal mucus on drug absorption, *Adv. Drug Delivery Rev.*, 1993, **11**, 201–220.

25 J. M. H. Larsson, K. A. Thomsson, A. M. Rodriguez-Pineiro, H. Karlsson and G. C. Hansson, Studies of mucus in mouse stomach, small intestine, and colon. III. Gastrointestinal Muc5ac and Muc2 mucin O-glycan pat-

terns reveal a regiospecific distribution, *Am. J. Physiol.: Gastrointest. Liver Physiol.*, 2013, **305**, G357–G363.

26 J. Cao, X. Chen, J. Liang, X.-Q. Yu, A.-L. Xu, E. Chan, W. Duan, M. Huang, J.-Y. Wen, X.-Y. Yu, X.-T. Li, F.-S. Sheu and S.-F. Zhou, Role of P-glycoprotein in the intestinal absorption of glabridin, an active flavonoid from the root of *Glycyrrhiza glabra*, *Drug Metab. Dispos.*, 2007, **35**, 539–553.

27 M. B. Baghdadi and T.-H. Kim, Analysis of mouse intestinal organoid culture with conditioned media isolated from mucosal enteric glial cells, *STAR Protoc.*, 2022, **3**, 101351.

28 N. Petersen, F. Reimann, S. Bartfeld, H. F. Farin, F. C. Ringnalda, R. G. J. Vries, S. van den Brink, H. Clevers, F. M. Gribble and E. J. P. de Koning, Generation of L Cells in Mouse and Human Small Intestine Organoids, *Diabetes*, 2014, **63**, 410–420.

29 J. von Moltke, M. Ji, H.-E. Liang and R. M. Locksley, Tuft-cell-derived IL-25 regulates an intestinal ILC2-epithelial response circuit, *Nature*, 2016, **529**, 221–225.

30 Y. Pei, L. Yue, W. Zhang, J. Xiang, Z. Ma and J. Han, Murine pluripotent stem cells that escape differentiation inside teratomas maintain pluripotency, *PeerJ*, 2018, **6**, e4177.

31 N. van der Wielen, M. van Avesaat, N. J. de Wit, J. T. Vogels, F. Troost, A. Masclee, S.-J. Koopmans, J. van der Meulen, M. V. Boekschoten, M. Muller, H. F. Hendriks, R. F. Witkamp and J. Meijerink, Cross-species comparison of genes related to nutrient sensing mechanisms expressed along the intestine, *PLoS One*, 2014, **9**, e107531.

32 M. Shigeta, N. Sanzen, M. Ozawa, J. Gu, H. Hasegawa and K. Sekiguchi, CD151 regulates epithelial cell–cell adhesion through PKC-and Cdc42-dependent actin cytoskeletal reorganization, *J. Cell Biol.*, 2003, **163**, 165–176.

33 S. J. Hao, Q. J. Fan, Y. Q. Bai, H. Fang, J. R. Zhou, T. Fukuda, J. G. Gu, M. Li and W. Z. Li, Core Fucosylation of Intestinal Epithelial Cells Protects Against *Salmonella Typhi* Infection via Up-Regulating the Biological Antagonism of Intestinal Microbiota, *Front. Microbiol.*, 2020, **11**, 1097.

34 J. M. Pickard, C. F. Maurice, M. A. Kinnebrew, M. C. Abt, D. Schenten, T. V. Golovkina, S. R. Bogatyrev, R. F. Ismagilov, E. G. Pamer, P. J. Turnbaugh and A. V. Chervonsky, Rapid fucosylation of intestinal epithelium sustains host-commensal symbiosis in sickness, *Nature*, 2014, **514**, 638–641.

35 B. Creamer, R. G. Shorter and J. Bamforth, The turnover and shedding of epithelial cells. I. The turnover in the gastro-intestinal tract, *Gut*, 1961, **2**, 110–118.

36 M. G. M. van de Schans, T. F. H. Bovee, G. M. Stoopen, M. Lorist, H. Gruppen and J.-P. Vincken, Prenylation and Backbone Structure of Flavonoids and Isoflavonoids from Licorice and Hop Influence Their Phase I and II Metabolism, *J. Agric. Food Chem.*, 2015, **63**, 10628–10640.

37 Q. Wang, X. Qiao, C.-F. Liu, S. Ji, L.-M. Feng, Y. Qian, D.-A. Guo and M. Ye, Metabolites identification of glycycoumarin, a major bioactive coumarin from licorice in rats, *J. Pharm. Biomed. Anal.*, 2014, **98**, 287–295.

38 A. Ermund, A. Schutte, M. E. V. Johansson, J. K. Gustafsson and G. C. Hansson, Studies of mucus in mouse stomach, small intestine, and colon. I. Gastrointestinal mucus layers have different properties depending on location as well as over the Peyer's patches, *Am. J. Physiol.: Gastrointest. Liver Physiol.*, 2013, **305**, G341–G347.

39 B. Myagmarjalbuu, M. J. Moon, S. H. Heo, S. I. Jeong, J.-S. Park, J. Y. Jun, Y. Y. Jeong and H. K. Kang, Establishment of a Protocol for Determining Gastrointestinal Transit Time in Mice Using Barium and Radiopaque Markers, *Korean J. Radiol.*, 2013, **14**, 45–50.

40 C. X. Pan, X. Y. Liu, Y. T. Zheng, Z. J. Zhang, Y. L. Li, B. Che, G. R. Liu, L. Y. Zhang, C. Z. Dong, H. A. Aisa, Z. Y. Du and Z. Q. Yuan, The mechanisms of melanogenesis inhibition by glabridin: molecular docking, PKA/MITF and MAPK/MITF pathways, *Food Sci. Hum. Wellness*, 2023, **12**, 212–222.

41 X. H. Song, S. T. Yin, Y. Z. Huo, M. Liang, L. H. Fan, M. Ye and H. B. Hu, Glycycoumarin ameliorates alcohol-induced hepatotoxicity via activation of Nrf2 and autophagy, *Free Radical Biol. Med.*, 2015, **89**, 135–146.

42 L. F. B. Bortolotto, F. R. Barbosa, G. Silva, T. A. Bitencourt, R. O. Beleboni, S. J. Baek, M. Marins and A. L. Fachin, Cytotoxicity of trans-chalcone and licochalcone A against breast cancer cells is due to apoptosis induction and cell cycle arrest, *Biomed. Pharmacother.*, 2017, **85**, 425–433.

43 D. Cevik, S. B. Yilmazgoz, Y. Kan, E. A. Guzelcan, I. Durmaz, R. Cetin-Atalay and H. Kirmizibekmez, Bioactivity-guided isolation of cytotoxic secondary metabolites from the roots of *Glycyrrhiza glabra* and elucidation of their mechanisms of action, *Ind. Crops Prod.*, 2018, **124**, 389–396.

44 M.-J. Hsieh, C.-W. Lin, S.-F. Yang, M.-K. Chen and H.-L. Chiou, Glabridin inhibits migration and invasion by transcriptional inhibition of matrix metalloproteinase 9 through modulation of NF-kappaB and AP-1 activity in human liver cancer cells, *Br. J. Pharmacol.*, 2014, **171**, 3037–3050.

45 Y. Fu, T. C. Hsieh, J. Q. Guo, J. Kunicki, M. Y. W. T. Lee, Z. Darzynkiewicz and J. M. Wu, Licochalcone-A, a novel flavonoid isolated from licorice root (*Glycyrrhiza glabra*), causes G2 and late-G1 arrests in androgen-independent PC-3 prostate cancer cells, *Biochem. Biophys. Res. Commun.*, 2004, **322**, 263–270.

46 X. H. Song, S. T. Yin, E. X. Zhang, L. H. Fan, M. Ye, Y. Zhang and H. B. Hu, Glycycoumarin exerts anti-liver cancer activity by directly targeting T-LAK cell-originated protein kinase, *Oncotarget*, 2016, **7**, 65732–65743.

47 Q. Wang, Y. Kuang, W. Song, Y. Qian, X. Qiao, D. Guo and M. Ye, Permeability through the Caco-2 cell monolayer of 42 bioactive compounds in the TCM formula Gegen-Qinlian Decoction by liquid chromatography tandem mass spectrometry analysis, *J. Pharm. Biomed. Anal.*, 2017, **146**, 206–213.

48 C. Araya-Cloutier, J.-P. Vincken, M. G. M. van de Schans, J. Hageman, G. Schaftenaar, H. M. W. den Bestens and

H. Gruppen, QSAR-based molecular signatures of prenylated (iso)flavonoids underlying antimicrobial potency against and membrane-disruption in Gram positive and Gram negative bacteria, *Sci. Rep.*, 2018, **8**, 9267.

49 M. Runge-Morris and T. A. Kocarek, Regulation of Sulfotransferase and UDP-Glucuronosyltransferase Gene Expression by the PPARs, *PPAR Res.*, 2009, **2009**, 728941.

50 M. J. Rein, M. Renouf, C. Cruz-Hernandez, L. Actis-Goretta, S. K. Thakkar and M. da Silva Pinto, Bioavailability of bioactive food compounds: a challenging journey to bioefficacy, *Br. J. Clin. Pharmacol.*, 2013, **75**, 588–602.

51 P. Zimniak, Detoxification reactions: Relevance to aging, *Ageing Res. Rev.*, 2008, **7**, 281–300.

52 T. Prueksaritanont, L. M. Gorham, J. H. Hochman, L. O. Tran and K. P. Vyas, Comparative studies of drug-metabolizing enzymes in dog, monkey, and human small intestines, and in Caco-2 cells, *Drug Metab. Dispos.*, 1996, **24**, 634–642.